Manuscript

Higher mortality rates leave heated ecosystem with similar size-structure despite larger, younger, and faster growing fish

Max Lindmark[a,1], Malin Karlsson[a], Anna Gårdmark[b]

[a] Swedish University of Agricultural Sciences, Department of Aquatic Resources, Institute of Coastal Research, Skolgatan 6, 742 42 Öregrund, Sweden

[b] Swedish University of Agricultural Sciences, Department of Aquatic Resources, Box 7018, 750 07 Uppsala, Sweden

[1] Author to whom correspondence should be addressed. Current address:
Max Lindmark, Swedish University of Agricultural Sciences, Department of Aquatic Resources, Institute of Marine Research, Turistgatan 5, 453 30 Lysekil, Sweden, Tel.: +46(0)104784137, email: max.lindmark@slu.se

Keywords: body growth, size-structure, size-spectrum, mortality, climate change, global warming, temperature

Abstract

Ectotherms are often predicted to "shrink" with global warming. This is in line with general growth models and the temperature-size rule (TSR), both predicting smaller adult sizes with warming. However, they also predict faster juvenile growth rates, leading to larger size-at-age of young organisms. Hence, the result of warming on the size-structure of a population depends on the interplay between how mortality rate, juvenile- and adult growth rates are affected by warming. In this study, we use time series of biological samples spanning more than two decades from a unique enclosed bay heated by cooling water from a nearby nuclear power plant to become +8C warmer than its reference area. We used growth-increment biochronologies (12658 reconstructed length-at-age estimates) to quantify how >20 years of warming has affected body growth and size-at-age and catch data to quantify mortality rates and population size-structure of Eurasian perch (*Perca fluviatilis*). In the heated area, growth rates were faster for all sizes, and hence size-at-age was larger for all ages, compared to the reference area. However, mortality rates were also higher, such that the difference in the size-spectrum exponent (describing the proportion of fish by size) was relatively minor and statistically uncertain. As such, our analysis reveals that mortality, in addition to plastic growth and size-responses, is a key factor determining the size structure of populations exposed to warming. Understanding the mechanisms by which warming affects the size-structure of populations is critical for prediction the impacts of climate change on ecological functions, interactions, and dynamics.

Significance statement

Ecosystem-scale warming experiments provide unique insight into potential impacts of climate change but are very rare. Our work utilizes an experimental set-up consisting of an enclosed bay heated by cooling water from a nuclear power plant for more than two decades, and a reference area. We analyze how changes in growth and mortality have affected the size- and age distribution in a common freshwater fish using time series of catch data and growth-increment biochronologies derived from their gill lids. Despite fish in the heated area being ~10% larger at a given age, elevated mortality rates have resulted in similar size structures. Accounting for the interplay between mortality and growth is key for predicting climate impacts on the size-structure of populations.

Introduction

Ectotherm species, constituting 99% of species globally (Wilson 1992; Atkinson & Sibly 1997), are commonly predicted to shrink in a warming world (Gardner *et al.* 2011; Sheridan & Bickford 2011; Cheung *et al.* 2013). Mean body size responses to temperature may however be uninformative, as the size-distribution of many species spans several orders of magnitude. For instance, warming can shift size-distributions without altering mean size if increases in juvenile size-at-age outweigh the decline in size-at-age in adults, which is consistent with the temperature size-rule, TSR (Atkinson 1994). Resolving how warming induces changes in population size-distributions may thus be more instructive (Fritschie & Olden 2016), especially for inferring warming effects on species' ecological role, biomass production, or energy fluxes (Yvon-Durocher *et al.* 2011). This is because key processes such as metabolism, feeding, growth, mortality scale with body size (Ursin 1967; Pauly 1980; Brown *et al.* 2004; Blanchard *et al.* 2017; Thorson *et al.* 2017; Andersen 2020). Hence, as the value of these traits at mean body size is not the same as the mean population trait value (Bernhardt *et al.* 2018), the size-distribution within a population matters for its dynamics and for how it changes under warming.

The population size distribution can be represented as a size-spectrum, which generally is the frequency distribution of individual body sizes (Edwards *et al.* 2017). It is often described in terms of the size-spectrum slope (slope of individuals or biomass of a size class over the mean size of that class on log-log scale (Sheldon *et al.* 1973; White *et al.* 2007; Edwards *et al.* 2017)) or simply the exponent of the power law individual size-distribution (Edwards *et al.* 2017). The size-spectrum thus results from temperature-dependent ecological processes such as body growth, mortality and recruitment (Blanchard *et al.* 2017; Heneghan *et al.* 2019). Despite its rich theoretical foundation (Andersen 2019) and usefulness as an ecological indicator (Blanchard *et al.* 2005), few studies have evaluated warming-effects on the species size-spectrum in larger bodied species (but see Blanchard *et al.*(2005)), and none in large scale

82 experimental set-ups. There are numerous paths by which a species' size-spectrum could
83 change with warming (Heneghan *et al.* 2019). For instance, in line with TSR predictions,
84 warming may lead to a smaller size-spectrum exponents (steeper slope) if the maximum size
85 declines. However, changes in size-at-age and the relative abundances of juveniles and adults
86 may alter this decline in the size-spectrum slope. Warming can also lead to elevated mortality
87 (Pauly 1980; Biro *et al.* 2007; Barnett *et al.* 2020; Berggren *et al.* 2021), which truncates the
88 age-distribution towards younger individuals (Barnett *et al.* 2017). This may reduce density
89 dependence and potentially increase growth rates, thus countering the effects of mortality on
90 the size spectrum exponent. However, not all sizes may benefit from warming, as e.g. the
91 optimum temperature for growth declines with size (Lindmark *et al.* 2022). Hence, the effect
92 of warming on the size-spectrum depends on several interlinked processes affecting
93 abundance-at-size and size-at-age.

94 Size-at-age is generally predicted to increase with warming for small individuals, but
95 decrease for large individuals according to the mentioned TSR (Atkinson 1994; Ohlberger
96 2013). Several factors likely contribute to this pattern, such as increased allocation to
97 reproduction (Wootton *et al.* 2022) and larger individuals in fish populations having optimum
98 growth rates at lower temperatures (Lindmark *et al.* 2022). Empirical support in fishes for this
99 pattern seem to be more consistent for increases in size-at-age of juveniles (Thresher *et al.*
100 2007; Rindorf *et al.* 2008; Huss *et al.* 2019) than declines in adult size-at-age (but see (Baudron
101 *et al.* 2014; Smoliński *et al.* 2020; Oke *et al.* 2022)), for which a larger diversity in responses
102 is observed among species (Barneche *et al.* 2019; e.g., Huss *et al.* 2019). However, most studies
103 have been done on commercially exploited species (since long time series are more common
104 in such species), which may confound effects of temperature plastic and/or genetic responses
105 to size-selective mortality on growth and size-at-age (Audzijonyte *et al.* 2016).

106 The effect of temperature on mortality rates of wild populations are more studied using
107 among-species analyses. These relationships based on thermal gradients in space may not
108 necessarily be the same as the effects of *warming* on mortality on single populations. Hence,
109 the effects of warming on growth and size-at-age and mortality within natural populations
110 constitute a key knowledge gap for predicting the consequences of climate change on
111 population size-spectra.

112 Here we used data from a unique, large-scale 23-year-long heating-experiment of a coastal
113 ecosystem to quantify how warming changed fish body growth, mortality, and the size structure
114 in an unexploited population of Eurasian perch (*Perca fluviatilis*, 'perch'). We compare fish
115 from this enclosed bay exposed to temperatures approximately 8°C above normal ('heated
116 area') with fish from a reference area in the adjacent archipelago (Fig. 1). Using hierarchical
117 Bayesian models, we quantify differences in key individual- and population level parameters,
118 such as body growth, asymptotic size, mortality rates, and size-spectra, between the heated and
119 reference coastal area.

120

121 ## Materials and Methods

122 *Data*

123 We use size-at-age data from perch sampled annually from an artificially heated enclosed bay
124 ('the Biotest basin') and its reference area, both in the western Baltic Sea (Fig. 1). Heating
125 started in 1980, the first analyzed cohort is 1981, and first and last catch year is 1987 and 2003,
126 respectively, to omit transient dynamics and acute responses, and to ensure we use cohorts that
127 only experienced one of the thermal environments during its life. A grid at the outlet of the
128 heated area (Fig. 1) prevented fish larger than 10 cm from migrating between the areas (Adill
129 *et al.* 2013; Huss *et al.* 2019), and genetic studies confirm the reproductive isolation between
130 the two populations during this time-period (Björklund *et al.* 2015). However, the grid was

131 removed in 2004, and since then fish growing up in the heated Biotest basin can easily swim
132 out, fish caught in the reference area cannot be assumed to be born there. Hence, we use data
133 only up until 2003. This resulted in 12658 length-at-age measurements from 2426 individuals
134 in 256 net deployments.

135 We use data from fishing events using survey-gillnets that took place in October in the
136 heated Biotest basin and in August in the reference area when temperatures are most
137 comparable between the two areas (Huss *et al.* 2019), because temperature affect catchability
138 in static gears. The catch was recorded by 2.5 cm length classes during 1987-2000, and into 1
139 cm length groups 2001-2003. To express lengths in a common length standard, 1 cm intervals
140 were converted into 2.5 cm intervals. The unit of catch data is hence the number of fish caught
141 by 2.5 cm size class per net per night (i.e., a catch-per-unit-effort [CPUE] variable). All data
142 from fishing events with disturbance affecting the catch (e.g., seal damage, strong algal growth
143 on the gears, clogging by drifting algae) were removed (years 1996 and 1999 from the heated
144 area in the catch data).

145 Length-at-age throughout life was reconstructed for a semi-random length-stratified subset
146 of caught individuals each year. This was done using growth-increment biochronologies
147 derived from annuli rings on the operculum bones (with control counts done on otoliths). Such
148 analyses have become increasingly used to analyze changes in growth and size-at-age of fishes
149 (Morrongiello & Thresher 2015; Essington *et al.* 2022). Specifically, an established power-law
150 relationship between the distance of annual rings and fish length was used: $L = \kappa R^s$, where L
151 is the length of the fish, R the operculum radius, κ the intercept, and s the slope of the line for
152 the regression of log-fish length on log-operculum radius from a large reference data set for
153 perch (Thoresson 1996). Back-calculated length-at-age were obtained from the relationship
154 $L_a = L_s(\frac{r_a}{R})^s$, where L_a is the back-calculated body length at age a, L_s is the final body length
155 (body length at catch), r_a is the distance from the center to the annual ring corresponding to

156 age a and $s = 0.861$ for perch (Thoresson 1996). Since perch exhibits sexual size-dimorphism,
157 and age-determination together with back calculation of growth was not done for males in all
158 years, we only used females for our analyses.
159
160 *Statistical Analysis*
161 The differences in size-at-age, growth, mortality, and size structure between perch in the heated
162 and the reference area were quantified using hierarchical linear and non-linear models fitted in
163 a Bayesian framework. First, we describe each statistical model and then provide details of
164 model fitting, model diagnostics and comparison.
165 We fit the von Bertalanffy growth equation (VBGE) (von Bertalanffy 1938; Beverton &
166 Holt 1957) on a log scale, describing length as a function of age to evaluate differences in size-
167 at-age and asymptotic size: $\log(L_t) = \log(L_\infty(1 - e^{(-K(t-t_0))}))$, where L_t is the length at age
168 (t, years), L_∞ is the asymptotic size, K is the Brody growth coefficient (yr^{-1}) and t_0 is the age
169 when the average length was zero. We used only age- and size-at-catch as the response
170 variables (i.e., not back-calculated length-at-age). This was to have a simpler model and not
171 have to account for parameters varying within individuals as well as cohorts, as mean sample
172 size per individual was only ~5. We let parameters vary among cohorts rather than year of
173 catch, because individuals within cohorts share similar environmental conditions and density
174 dependence (Morrongiello & Thresher 2015). Eight models in total were fitted (with area being
175 dummy-coded), with different combinations of shared and area-specific parameters. We
176 evaluated if models with area-specific parameters led to better fit and quantified the differences
177 in area-specific parameters (indexed by subscripts heat and ref). The model with all area-
178 specific parameter can be written as:

179 $$L_i \sim \text{Student-}t(\upsilon, \mu_i, \sigma) \quad (1)$$

180
$$\log(\mu_i) = A_{\text{ref}} \log\left[L_{\infty \text{ref}j[i]}\left(1 - e^{\left(-K_{\text{ref}j[i]}\left(t - t_{0\text{ref}j[i]}\right)\right)}\right)\right] + A_{\text{heat}} \log\left[L_{\infty \text{heat}j[i]}\left(1 - e^{\left(-K_{\text{heat}j[i]}\left(t - t_{0\text{heat}j[i]}\right)\right)}\right)\right] \quad (2)$$

181
$$\begin{bmatrix} L_{\infty \text{ref}j} \\ L_{\infty \text{heat}j} \\ K_{\text{ref}j} \\ K_{\text{heat}j} \end{bmatrix} \sim \text{MVNormal}\left(\begin{bmatrix} \mu_{L_{\infty \text{ref}}} \\ \mu_{L_{\infty \text{heat}}} \\ \mu_{K_{\text{ref}}} \\ \mu_{K_{\text{heat}}} \end{bmatrix}, \begin{bmatrix} \sigma_{L_{\infty \text{ref}}} & 0 & 0 & 0 \\ 0 & \sigma_{L_{\infty \text{heat}}} & 0 & 0 \\ 0 & 0 & \sigma_{K_{\text{ref}}} & 0 \\ 0 & 0 & 0 & \sigma_{K_{\text{heat}}} \end{bmatrix}\right) \quad (3)$$

182 where lengths are $Student\text{-}t$ distributed to account for extreme observations, υ, μ and ϕ
183 represent the degrees of freedom, mean and the scale parameter, respectively. A_{ref} and A_{heat}
184 are dummy variables such that $A_{\text{ref}} = 1$ and $A_{\text{heat}} = 0$ if it is the reference area, and vice versa
185 for the heated area. The multivariate normal distribution in Eq. 3 is the prior for the cohort-
186 varying parameters $L_{\infty \text{ref}j}$, $L_{\infty \text{heat}j}$, $K_{\text{ref}j}$ and $K_{\text{heat}j}$ (for cohorts $j = 1981,\ldots,1997$) (note that
187 cohorts extend further back in time than the catch data), with hyper-parameters $\mu_{L_{\infty \text{ref}}}$, $\mu_{L_{\infty \text{heat}}}$,
188 $\mu_{K_{\text{ref}}}$, $\mu_{K_{\text{heat}}}$ describing the non-varying population means and a covariance matrix with the
189 between-cohort variation along the diagonal (note we did not model a correlation between the
190 parameters, hence off-diagonals are 0). The other seven models include some or all parameters
191 as parameters common for the two areas, e.g., substituting $L_{\infty \text{ref}j}$ and $L_{\infty \text{heat}j}$ with $L_{\infty j}$. To aid
192 convergence of this non-linear model, we used informative priors chosen after visualizing
193 draws from prior predictive distributions (Wesner & Pomeranz 2021) using probable parameter
194 values (*Supporting Information*, Fig. S1, S7). We used the same prior distribution for each
195 parameter class for both areas to not introduce any other sources of differences in parameter
196 estimates between areas. We used the following priors for the VBGE model:
197 $\mu_{L_{\infty \text{ref,heat}}} \sim N(45,20)$, $\mu_{K_{\text{ref,heat}}} \sim N(0.2, 0.1)$, $t_{0\text{ref,heat}} \sim N(-0.5, 1)$ and $\upsilon \sim gamma(2,0.1)$. σ
198 parameters, $\mu_{L_{\infty \text{ref}}}$, $\mu_{L_{\infty \text{heat}}}$, $\mu_{K_{\text{ref}}}$, $\mu_{K_{\text{heat}}}$ were given a $Student - t(3,0,2.5)$ prior.

199 We also compared how body growth scales with body size (in contrast to length vs age).
200 This is because size-at-age reflects lifetime growth history rather than current growth histories

and may thus be large because growth was fast early in life, not because current growth rates are fast (Lorenzen 2016). We therefore fit allometric growth models describing how specific growth rate scales with length: $G = \alpha L^{\theta}$, where G, the annual specific growth between year t and $t+1$, is defined as: $G = 100 \times (log\ (L_{t+1})\ - log\ (L_t)\ )$ and L is the geometric mean length: $L = (L_{t+1} \times L_t)^{0.5}$. Here we also used back-calculated length-at-age, resulting in multiple observations for each individual. As with the VBGE model, we dummy coded area to compare models with different combinations of common and shared parameters. We assumed growth rates were $Student - t$ distributed, and the full model can be written as:

$$L_i \sim Student - t(v, \mu_i, \sigma) \quad (4)$$

$$\mu_i = A_{\text{ref}}\left(\alpha_{\text{ref}j[i],k[i]} L^{\theta_{\text{ref}}}\right) + A_{\text{heat}}\left(\alpha_{\text{heat}j[i],k[i]} L^{\theta_{\text{heat}}}\right) \quad (5)$$

$$\alpha_{\text{ref,heat}j} \sim N\left(\mu_{\alpha_{\text{ref,heat}j}}, \sigma_{\alpha_{\text{ref,heat}j}}\right) \quad (6)$$

$$\alpha_{\text{ref,heat}j} \sim N\left(\mu_{\alpha_{\text{ref,heat}j}}, \sigma_{\alpha_{\text{ref,heat}j}}\right) \quad (7)$$

$$\theta_{\text{ref,heat}j} \sim N\left(\mu_{\theta_{\text{ref,heat}j}}, \sigma_{\theta_{\text{ref,heat}j}}\right) \quad (8)$$

$$\theta_{\text{ref,heat}j} \sim N\left(\mu_{\theta_{\text{ref,heat}j}}, \sigma_{\theta_{\text{ref,heat}j}}\right) \quad (9)$$

We assumed only α varied across individuals j within cohorts k and compared two models: one with θ common for the heated and reference area, and one with an area-specific θ. We used the following priors, after visual exploration of the prior predictive distribution (*Supporting Information*, Fig. S8, S10): $\alpha_{\text{ref,heat}} \sim N(500, 100)$, $\theta_{\text{ref,heat}} \sim N(-1.2, 0.3)$ and $v \sim gamma(2, 0.1)$. σ, $\sigma_{\text{id:cohort}}$ and σ_{cohort} were all given a $Student - t(3, 0, 13.3)$ prior.

We estimated total mortality by fitting linear models to the natural log of catch (CPUE) as a function of age (catch curve regression), under the assumption that in a closed population, the exponential decline can be described as $N_t = N_0 e^{-Zt}$, where N_t is the population at time t, N_0 is the initial population size and Z is the instantaneous mortality rate. This equation can be rewritten as a linear equation: $log\ (C_t)\ = log\ (vN_0)\ - Zt$, where C_t is catch at age t, if catch is assumed proportional to the number of fish (i.e., $C_t = vN_t$). Hence, the negative of the slope of the regression is the mortality rate, Z. To get catch-at-age data, we constructed area-specific

age-length keys using the sub-sample of the total (female) catch that was age-determined. Age length-keys describe the age-proportions of each length-category (i.e., a matrix with length category as rows, ages as columns). Age composition is then estimated for the total catch based on the "probability" of fish in each length-category being a certain age. With fit this model with and without an $age \times area$-interaction, and the former can be written as:

$$\log(CPUE_i) \sim \text{Student-}t(\upsilon, \mu_i, \sigma) \tag{10}$$

$$\mu_i = \beta_{0j[i]}(area_{\text{ref}}) + \beta_{1j[i]}(area_{\text{heat}}) + \beta_{2j[i]} age + \beta_{3j[i]}(age \times area_{\text{heat}}) \tag{11}$$

$$\begin{bmatrix} \beta_{0j} \\ \beta_{1j} \\ \beta_{2j} \\ \beta_{3j} \end{bmatrix} \sim \text{MVNormal}\left(\begin{bmatrix} \mu_{\beta_0} \\ \mu_{\beta_1} \\ \mu_{\beta_2} \\ \mu_{\beta_3} \end{bmatrix}, \begin{bmatrix} \sigma_{\beta_0} & 0 & 0 & 0 \\ 0 & \sigma_{\beta_1} & 0 & 0 \\ 0 & 0 & \sigma_{\beta_2} & 0 \\ 0 & 0 & 0 & \sigma_{\beta_3} \end{bmatrix} \right) \tag{12}$$

where β_{0j} and β_{1j} are the intercepts for the reference and heated areas, respectively, β_{2j} is the age slope for the reference area and β_{3j} is the interaction between age and $area$. All parameters vary by cohort (for cohort $j = 1981, \ldots, 2000$) and their correlation is set to 0 (Eq. 12). We use the following (vague) priors: $\mu_{\beta_{0,\ldots,3j}} \sim N(0, 10)$ (where μ_{β_2} is the population-level estimate for $-Z_{\text{ref}}$ and $\mu_{\beta_2} + \mu_{\beta_3}$ is the population-level estimate for $-Z_{\text{heat}}$) and $\upsilon \sim gamma(2,0.1)$. σ and $\sigma_{\beta_{0,\ldots,3}}$ were given a $Student - t(3,0,2.5)$ prior.

Lastly, we quantified differences in the size-distributions between the areas using size-spectrum exponents. We estimate the biomass size-spectrum exponent γ directly, using the likelihood approach for binned data, i.e., the *MLEbin* method in the R package *sizeSpectra* (Edwards *et al.* 2017, 2020; Edwards 2020). This method explicitly accounts for uncertainty in body masses *within* size-classes (bins) in the data and has been shown to be less biased than regression-based methods or the likelihood method based on bin-midpoints (Edwards *et al.* 2017, 2020). We pooled all years to ensure negative relationships between biomass and size in the size-classes (as the sign of the relationship varied between years).

All analyses were done using R (R Core Team 2020) version 4.0.2 with R Studio (2021.09.1). The packages within the *tidyverse* (Wickham *et al.* 2019) collection were used to processes and visualize data. Models where fit using the R package *brms* (Bürkner 2017). When priors were not chosen based on the prior predictive distributions, we used the default priors from *brms* as written above. We used 3 chains and 4000 iterations in total per chain. Models were compared by evaluating their expected predictive accuracy (expected log pointwise predictive density) using leave-one-out cross-validation (LOO-CV) (Vehtari *et al.* 2017) while ensuring Pareto k values < 0.7, in the R package *loo* (Vehtari *et al.* 2020). Results of the model comparison can be found in the *Supporting Information*, Table S1-S2. We used *bayesplot* (Gabry *et al.* 2019) and *tidybayes* (Kay 2019) to process and visualize model diagnostics and posteriors. Model convergence and fit was assessed by ensuring potential scale reduction factors ($\hat{R}$) were less than 1.1, suggesting all three chains converged to a common distribution) (Gelman *et al.* 2003), and by visually inspecting trace plots, residuals QQ-plots and with posterior predictive checks (*Supporting Information*, Fig. S2, S9, S11).

Results

Analysis of fish (perch) size-at-age using the von Bertalanffy growth equation (VBGE) revealed that fish cohorts (year classes) in the heated area both grew faster initially (larger size-at-age and VBGE K parameter) and reached larger predicted asymptotic sizes than those in the unheated reference area (Fig. 2). The model with area-specific VBGE parameters (L_∞, K and t_0) had best out of sample predictive accuracy (the largest expected log pointwise predictive density for a new observation; Table S1), and there is a clear difference in both the estimated values for fish asymptotic length (L_∞) and growth rate (K) between the heated and reference area (Fig. 2B-E). For instance, the distribution of differences between the heated and reference area of the posterior samples for L_∞ and K only had 11% and 2%, respectively, of the density

below 0, illustrating that it is likely that the parameters are larger in the heated area (Fig. 2C, E). We estimated that the asymptotic length of fish in the heated area was 1.16 times larger than in the reference area ($L_{\infty\text{heat}} = 45.7[36.8, 56.3]$, $L_{\infty\text{ref}} = 39.4[35.4, 43.9]$, where the point estimate is the posterior median and values in brackets correspond to the 95% credible interval). The growth coefficient was 1.27 times larger in the heated area ($K_{\text{heat}} = 0.19[0.15, 0.23], K_{\text{ref}} = 0.15[0.12, 0.17]$). Also $t_{0\text{heat}}$ was larger than $t_{0\text{ref}}$ ($-0.16[-0.21, -0.11]$ vs $-0.44[-0.56, -0.33]$, respectively). These differences in growth parameters lead to fish being approximately 10% larger in the heated area relative to the reference area (Fig. S4).

In addition, we found that growth rates in the reference area were both slower and declined faster with size compared to the heated area (Fig. 3). The best model for growth ($G = \alpha L^{\theta}$) had area-specific α and θ parameters (Table S2). Initial growth (α) was estimated to be 1.18 times faster in the heated than in the reference area ($\alpha_{\text{heat}} = 509.7[460.1,563.5], \alpha_{\text{ref}} = 433.5[413.3,454.1]$), and growth of fish in the heated area decline more slowly with length than in the reference area ($\theta_{\text{heat}} = -1.13[-1.16, -1.11], \theta_{\text{ref}} = -1.18[-1.19, -1.16]$). The distribution of differences of the posterior samples for α and θ both only had 0.3% of the density below 0 (Fig. 3C, E), indicating high probability that length-based growth rates are faster in the heated area.

By analyzing the decline in catch-per-unit-effort over age, we found that the instantaneous mortality rate Z (rate at which log abundance declines with age) is higher in the heated area (Fig. 4). The overlap with zero is 0.05% for the distribution of differences of posterior samples of Z_{heat} and Z_{ref} (Fig. 4C). We estimated Z_{heat} to be $0.7[0.67,0.82]$ and Z_{ref} to be $0.63[0.57,0.68]$, which corresponds to annual mortality rates of 53% in the heated area and 47% in the reference area.

Lastly, analysis of the size-structure in the two areas revealed that, despite the faster growth rates and larger sizes in the heated area for fish of all sizes, the higher mortality rates in the heated area led to largely similar size-structures. Specifically, while largest fish were found in the heated area, the size-spectrum exponent was only slightly larger in the heated area (Fig. 5A), and their 95% confidence intervals largely overlap (Fig. 5C).

Discussion

Our study provides strong evidence for warming-induced differentiation in growth, mortality, and size-structure in a natural population of an unexploited, temperate fish species exposed to an ecosystem-scale experiment with 5-10 ℃ above normal temperatures for more than two decades. While it is a study on only a single species, these features make it a unique climate change experiment, as experimental studies on fish to date are much shorter and often on scales much smaller than whole ecosystems, and long time series of biological samples exist mainly for commercially exploited fish species (Thresher *et al.* 2007; Baudron *et al.* 2014; Smoliński *et al.* 2020) (in which fisheries exploitation affects size-structure both directly and indirectly by selecting for fast growing individuals). While factors other than temperature could have contributed to the observed elevated growth and mortality, the temperature contrast is unusually large for natural systems (i.e., 5-10 ℃, which can be compared to the 1.35 ℃ change in the Baltic Sea between 1982 and 2006 (Belkin 2009)). Moreover, heating occurred at the scale of a whole ecosystem, which makes the findings highly relevant in the context of global warming.

Interestingly, our findings contrast with both broader predictions about declining mean or adult body sizes based on the GOLT hypothesis (Cheung *et al.* 2013; Pauly 2021), and with intraspecific patterns such as the TSR (temperature-size rule (1994)). The contrasts lie in that both asymptotic size and size-at-age of mature individuals, as well as the proportion of larger

325 individuals were slightly larger and higher in the heated area—despite the elevated mortality
326 rates. This result was unexpected for two reasons: optimum growth temperatures generally
327 decline with body size within species under food satiation in experimental studies (Lindmark
328 *et al.* 2022), and fish tend to mature at smaller body size and allocate more energy into
329 reproduction as it gets warmer (Wootton *et al.* 2022). Both patterns have been used to explain
330 how growth can increase for small and young fish, while large and old fish typically do not
331 benefit from warming. Our study species is no exception to these rules (Karås & Thoresson
332 1992; Sandström *et al.* 1995; Huss *et al.* 2019). This suggests that growth dynamics under food
333 satiation may not be directly proportional to those under natural feeding conditions (Railsback
334 2022). Moreover, our results suggest that growth changes emerge not only from direct
335 physiological responses to increased temperatures, but also from warming-induced changes in
336 the food web, e.g., prey productivity, diet composition and trophic transfer efficiencies
337 (Gårdmark & Huss 2020). It also highlights that we need to focus on understanding to what
338 extent the commonly observed increase in size-at-age for juveniles in warm environments can
339 be maintained as they grow older.

340 Our finding that mortality rates were higher in the heated area was expected—warming
341 leads to faster metabolic rates, which in turn is associated with shorter life span (Brown *et al.*
342 2004; McCoy & Gillooly 2008; Munch & Salinas 2009) (higher "physiological" mortality).
343 Warming may also increase predation mortality, as predators' feeding rates increase in order
344 to meet the higher demand of food (Ursin 1967; Pauly 1980; Biro *et al.* 2007). However, most
345 evidence to date of the temperature dependence of mortality rates in natural populations stem
346 from across species studies (Pauly 1980; Gislason *et al.* 2010; Thorson *et al.* 2017) (but see
347 (Biro *et al.* 2007; Berggren *et al.* 2021)). Across species relationships are not necessarily
348 determined by the same processes as within species relationships; thus, our finding of warming-

induced mortality in a heated vs control environment in two nearby con-specific populations is important.

Since a key question for understanding the implications of warming on ectotherm populations is if larger individuals in a population become rarer or smaller (Ohlberger 2013; Ohlberger *et al.* 2018), within-species mortality and growth responses to warming need further study. Importantly, this requires accounting also for effects of warming on growth, and how responses in growth and mortality depend on each other. For instance, higher mortality (predation or natural, physiological mortality) can release intra-specific competition and thus increase growth. Conversely, altered growth and body sizes can lead to changes in size-specific mortality, such as predation or starvation. In conclusion, individual-level patterns such as the TSR may be of limited use for predicting changes on the population-level size structure as it does not concern changes in abundance-at-size via mortality. Mortality may, however, be an important driver of the observed shrinking of ectotherms (Peralta-Maraver & Rezende 2021). Understanding the mechanisms by which the size- and age-distribution change with warming is critical for predicting how warming changes species functions and ecological roles (Fritschie & Olden 2016; Audzijonyte *et al.* 2020; Gårdmark & Huss 2020). Our findings demonstrate that a key to do this is to acknowledge temperature effects on both growth and mortality and how they interact.

Acknowledgements

We thank all staff involved in data collection, and Jens Olsson and Göran Sundblad for discussion. This study was supported by SLU Quantitative Fish and Fisheries Ecology.

Code and Data Availability

All data and R code to reproduce the analyses can be downloaded from a GitHub repository (https://github.com/maxlindmark/warm_life_history) and will be archived on Zenodo upon publication. Researchers interested in using the data for purposes other than replicating our analyses are advised to request the data from the authors, as other useful information from the original data might not be included.

Author Contributions

ML conceived the idea and designed the study and the statistical analysis. Data-processing, initial statistical analyses, and initial writing was done by MK and ML. AG contributed critically to all mentioned parts of the paper. All authors contributed to the manuscript writing and gave final approval for publication.

References

Adill, A., Mo, K., Sevastik, A., Olsson, J. & Bergström, L. (2013). *Biologisk recipientkontroll vid Forsmarks kärnkraftverk (in Swedish)* (Rapport No. 2013:19). Öregrund.

Andersen, K.H. (2019). *Fish Ecology, Evolution, and Exploitation: A New Theoretical Synthesis*. Princeton University Press.

Andersen, K.H. (2020). Size-based theory for fisheries advice. *ICES J Mar Sci*, 77, 2445–2455.

Atkinson, D. (1994). Temperature and organism size—A biological law for ectotherms? *Advances in Ecological Research*, 25, 1–58.

Atkinson, D. & Sibly, R.M. (1997). Why are organisms usually bigger in colder environments? Making sense of a life history puzzle. *Trends in Ecology & Evolution*, 12, 235–239.

Audzijonyte, A., Fulton, E., Haddon, M., Helidoniotis, F., Hobday, A.J., Kuparinen, A., *et al.* (2016). Trends and management implications of human-influenced life-history changes in marine ectotherms. *Fish and Fisheries*, 17, 1005–1028.

Audzijonyte, A., Richards, S.A., Stuart-Smith, R.D., Pecl, G., Edgar, G.J., Barrett, N.S., *et al.* (2020). Fish body sizes change with temperature but not all species shrink with warming. *Nat Ecol Evol*, 4, 809–814.

Barneche, D.R., Jahn, M. & Seebacher, F. (2019). Warming increases the cost of growth in a model vertebrate. *Functional Ecology*, 33, 1256–1266.

Barnett, H.K., Quinn, T.P., Bhuthimethee, M. & Winton, J.R. (2020). Increased prespawning mortality threatens an integrated natural- and hatchery-origin sockeye salmon population in the Lake Washington Basin. *Fisheries Research*, 227, 105527.

Barnett, L.A.K., Branch, T.A., Ranasinghe, R.A. & Essington, T.E. (2017). Old-Growth Fishes Become Scarce under Fishing. *Current Biology*, 27, 2843-2848.e2.

Baudron, A.R., Needle, C.L., Rijnsdorp, A.D. & Marshall, C.T. (2014). Warming temperatures and smaller body sizes: synchronous changes in growth of North Sea fishes. *Global Change Biology*, 20, 1023–1031.

Belkin, I.M. (2009). Rapid warming of large marine ecosystems. *Progress in Oceanography*, 81, 207–213.

Berggren, T., Bergström, U., Sundblad, G. & Östman, Ö. (2021). Warmer water increases early body growth of northern pike (Esox lucius) but mortality has larger impact on decreasing body sizes. *Can. J. Fish. Aquat. Sci.*

Bernhardt, J.R., Sunday, J.M., Thompson, P.L. & O'Connor, M.I. (2018). Nonlinear averaging of thermal experience predicts population growth rates in a thermally variable environment. *Proceedings of the Royal Society B: Biological Sciences*, 285, 20181076.

von Bertalanffy, L. (1938). A quantitative theory of organic growth (inquiries on growth laws. II). *Human Biology*, 10, 181–213.

Beverton, R.J.H. & Holt, S.J. (1957). *On the Dynamics of Exploited Fish Populations*. Fishery Investigations London Series 2, Volume 19.

Biro, P.A., Post, J.R. & Booth, D.J. (2007). Mechanisms for climate-induced mortality of fish populations in whole-lake experiments. *Proceedings of the National Academy of Sciences*, 104, 9715–9719.

Björklund, M., Aho, T. & Behrmann-Godel, J. (2015). Isolation over 35 years in a heated biotest basin causes selection on MHC class IIß genes in the European perch (Perca fluviatilis L.). *Ecol Evol*, 5, 1440–1455.

Blanchard, J.L., Dulvy, N., Jennings, S., Ellis, J., Pinnegar, J., Tidd, A., *et al.* (2005). Do climate and fishing influence size-based indicators of Celtic Sea fish community structure? *ICES Journal of Marine Science*, 62, 405–411.

Blanchard, J.L., Heneghan, R.F., Everett, J.D., Trebilco, R. & Richardson, A.J. (2017). From bacteria to whales: Using functional size spectra to model marine ecosystems. *Trends in Ecology & Evolution*, 32, 174–186.

Brown, J.H., Gillooly, J.F., Allen, A.P., Savage, V.M. & West, G.B. (2004). Toward a metabolic theory of ecology. *Ecology*, 85, 1771–1789.

Bürkner, P.-C. (2017). **brms** : An *R* Package for Bayesian Multilevel Models Using *Stan*. *Journal of Statistical Software*, 80.

Cheung, W.W.L., Sarmiento, J.L., Dunne, J., Frölicher, T.L., Lam, V.W.Y., Deng Palomares, M.L., *et al.* (2013). Shrinking of fishes exacerbates impacts of global ocean changes on marine ecosystems. *Nature Climate Change*, 3, 254–258.

Edwards, A. (2020). sizeSpectra: Fitting Size Spectra to Ecological Data Using Maximum Likelihood.

Edwards, A.M., Robinson, J.P.W., Blanchard, J.L., Baum, J.K. & Plank, M.J. (2020). Accounting for the bin structure of data removes bias when fitting size spectra. *Marine Ecology Progress Series*, 636, 19–33.

Edwards, A.M., Robinson, J.P.W., Plank, M.J., Baum, J.K. & Blanchard, J.L. (2017). Testing and recommending methods for fitting size spectra to data. *Methods in Ecology and Evolution*, 8, 57–67.

Essington, T.E., Matta, M.E., Black, B.A., Helser, T.E. & Spencer, P.D. (2022). Fitting growth models to otolith increments to reveal time-varying growth. *Can. J. Fish. Aquat. Sci.*, 79, 159–167.

Fritschie, K.J. & Olden, J.D. (2016). Disentangling the influences of mean body size and size structure on ecosystem functioning: an example of nutrient recycling by a non-native crayfish. *Ecology and Evolution*, 6, 159–169.

Gabry, J., Simpson, D., Vehtari, A., Betancourt, M. & Gelman, A. (2019). Visualization in Bayesian workflow. *J. R. Stat. Soc. A*, 182, 389–402.

Gårdmark, A. & Huss, M. (2020). Individual variation and interactions explain food web responses to global warming. *Philosophical Transactions of the Royal Society B: Biological Sciences*, 375, 20190449.

Gardner, J.L., Peters, A., Kearney, M.R., Joseph, L. & Heinsohn, R. (2011). Declining body size: a third universal response to warming? *Trends in Ecology & Evolution*, 26, 285–291.

Gelman, A., Carlin, J., Stern, H. & Rubin, D. (2003). *Bayesian Data Analysis. 2nd edition*. Chapman and Hall/CRC, Boca Raton.

Gislason, H., Daan, N., Rice, J.C. & Pope, J.G. (2010). Size, growth, temperature and the natural mortality of marine fish: Natural mortality and size. *Fish and Fisheries*, 11, 149–158.

Heneghan, R.F., Hatton, I.A. & Galbraith, E.D. (2019). Climate change impacts on marine ecosystems through the lens of the size spectrum. *Emerging Topics in Life Sciences*, 3, 233–243.

Huss, M., Lindmark, M., Jacobson, P., van Dorst, R.M. & Gårdmark, A. (2019). Experimental evidence of gradual size-dependent shifts in body size and growth of fish in response to warming. *Glob Change Biol*, 25, 2285–2295.

Karås, P. & Thoresson, G. (1992). An application of a bioenergetics model to Eurasian perch (Perca fluviatilis L.). *Journal of Fish Biology*, 41, 217–230.

Kay, M. (2019). tidybayes: Tidy Data and Geoms for Bayesian Models.

Lindmark, M., Ohlberger, J. & Gårdmark, A. (2022). Optimum growth temperature declines with body size within fish species. *Global Change Biology*, 28, 2259–2271.

Lorenzen, K. (2016). Toward a new paradigm for growth modeling in fisheries stock assessments: Embracing plasticity and its consequences. *Fisheries Research*, Growth: theory, estimation, and application in fishery stock assessment models, 180, 4–22.

McCoy, M.W. & Gillooly, J.F. (2008). Predicting natural mortality rates of plants and animals. *Ecology Letters*, 11, 710–716.

Morrongiello, J.R. & Thresher, R.E. (2015). A statistical framework to explore ontogenetic growth variation among individuals and populations: a marine fish example. *Ecological Monographs*, 85, 93–115.

Munch, S.B. & Salinas, S. (2009). Latitudinal variation in lifespan within species is explained by the metabolic theory of ecology. *Proceedings of the National Academy of Sciences*, 106, 13860–13864.

Ohlberger, J. (2013). Climate warming and ectotherm body size – from individual physiology to community ecology. *Functional Ecology*, 27, 991–1001.

Ohlberger, J., Ward, E.J., Schindler, D.E. & Lewis, B. (2018). Demographic changes in Chinook salmon across the Northeast Pacific Ocean. *Fish and Fisheries*, 19, 533–546.

Oke, K.B., Mueter, F.J. & Litzow, M.A. (2022). Warming leads to opposite patterns in weight-at-age for young versus old age classes of Bering Sea walleye pollock. *Can. J. Fish. Aquat. Sci.*

Pauly, D. (1980). On the interrelationships between natural mortality, growth parameters, and mean environmental temperature in 175 fish stocks. *ICES Journal of Marine Science*, 39, 175–192.

Pauly, D. (2021). The gill-oxygen limitation theory (GOLT) and its critics. *Science Advances*, 7, eabc6050.

Peralta-Maraver, I. & Rezende, E.L. (2021). Heat tolerance in ectotherms scales predictably with body size. *Nat. Clim. Chang.*, 11, 58–63.

R Core Team. (2020). *R: A Language and Environment for Statistical Computing. R Foundation for Statistical Computing*. Vienna, Austria.

Railsback, S.F. (2022). What We Don't Know About the Effects of Temperature on Salmonid Growth. *Transactions of the American Fisheries Society*, 151, 3–12.

Rindorf, A., Jensen, H. & Schrum, C. (2008). Growth, temperature, and density relationships of North Sea cod (Gadus morhua). *Canadian Journal of Fisheries and Aquatic Sciences*, 65, 456–470.

Sandström, O., Neuman, E. & Thoresson, G. (1995). Effects of temperature on life history variables in perch. *Journal of Fish Biology*, 47, 652–670.

Sheldon, R.W., Sutcliffe, W.H. & Prakash, A. (1973). The Production of Particles in the Surface Waters of the Ocean with Particular Reference to the Sargasso Sea1. *Limnology and Oceanography*, 18, 719–733.

Sheridan, J.A. & Bickford, D. (2011). Shrinking body size as an ecological response to climate change. *Nature Climate Change*, 1, 401–406.

Smoliński, S., Deplanque-Lasserre, J., Hjörleifsson, E., Geffen, A.J., Godiksen, J.A. & Campana, S.E. (2020). Century-long cod otolith biochronology reveals individual growth plasticity in response to temperature. *Sci Rep*, 10, 16708.

Thoresson, G. (1996). *Metoder för övervakning av kustfiskbestånd (in Swedish)* (No. 3). Kustrapport. Kustlaboratoriet, Fiskeriverket, Öregrund.

Thorson, J.T., Munch, S.B., Cope, J.M. & Gao, J. (2017). Predicting life history parameters for all fishes worldwide. *Ecological Applications*, 27, 2262–2276.

Thresher, R.E., Koslow, J.A., Morison, A.K. & Smith, D.C. (2007). Depth-mediated reversal of the effects of climate change on long-term growth rates of exploited marine fish. *Proceedings of the National Academy of Sciences, USA*, 104, 7461–7465.

Ursin, E. (1967). A Mathematical Model of Some Aspects of Fish Growth, Respiration, and Mortality. *Journal of the Fisheries Research Board of Canada*, 24, 2355–2453.

Vehtari, A., Gabry, J., Magnusson, M., Yao, Y., Bürkner, P., Paananen, T., *et al.* (2020). loo: Efficient leave-one-out cross-validation and WAIC for Bayesian models.

Vehtari, A., Gelman, A. & Gabry, J. (2017). Practical Bayesian model evaluation using leave-one-out cross-validation and WAIC. *Stat Comput*, 27, 1413–1432.

Wesner, J.S. & Pomeranz, J.P.F. (2021). Choosing priors in Bayesian ecological models by simulating from the prior predictive distribution. *Ecosphere*, 12, e03739.

White, E.P., Ernest, S.K.M., Kerkhoff, A.J. & Enquist, B.J. (2007). Relationships between body size and abundance in ecology. *Trends in Ecology & Evolution*, 22, 323–330.

Wickham, H., Averick, M., Bryan, J., Chang, W., D'Agostino McGowan, L., François, R., *et al.* (2019). Welcome to the tidyverse. *Journal of Open Source Software*, 1686.

Wilson, E.O. (1992). *The Diversity of Life*. Harvard University Press, Cambridge.

Wootton, H.F., Morrongiello, J.R., Schmitt, T. & Audzijonyte, A. (2022). Smaller adult fish size in warmer water is not explained by elevated metabolism. *Ecology Letters*, 25, 1177–1188.

Yvon-Durocher, G., Montoya, J.M., Trimmer, M. & Woodward, G. (2011). Warming alters the size spectrum and shifts the distribution of biomass in freshwater ecosystems. *Global Change Biology*, 17, 1681–1694.

555 Figures

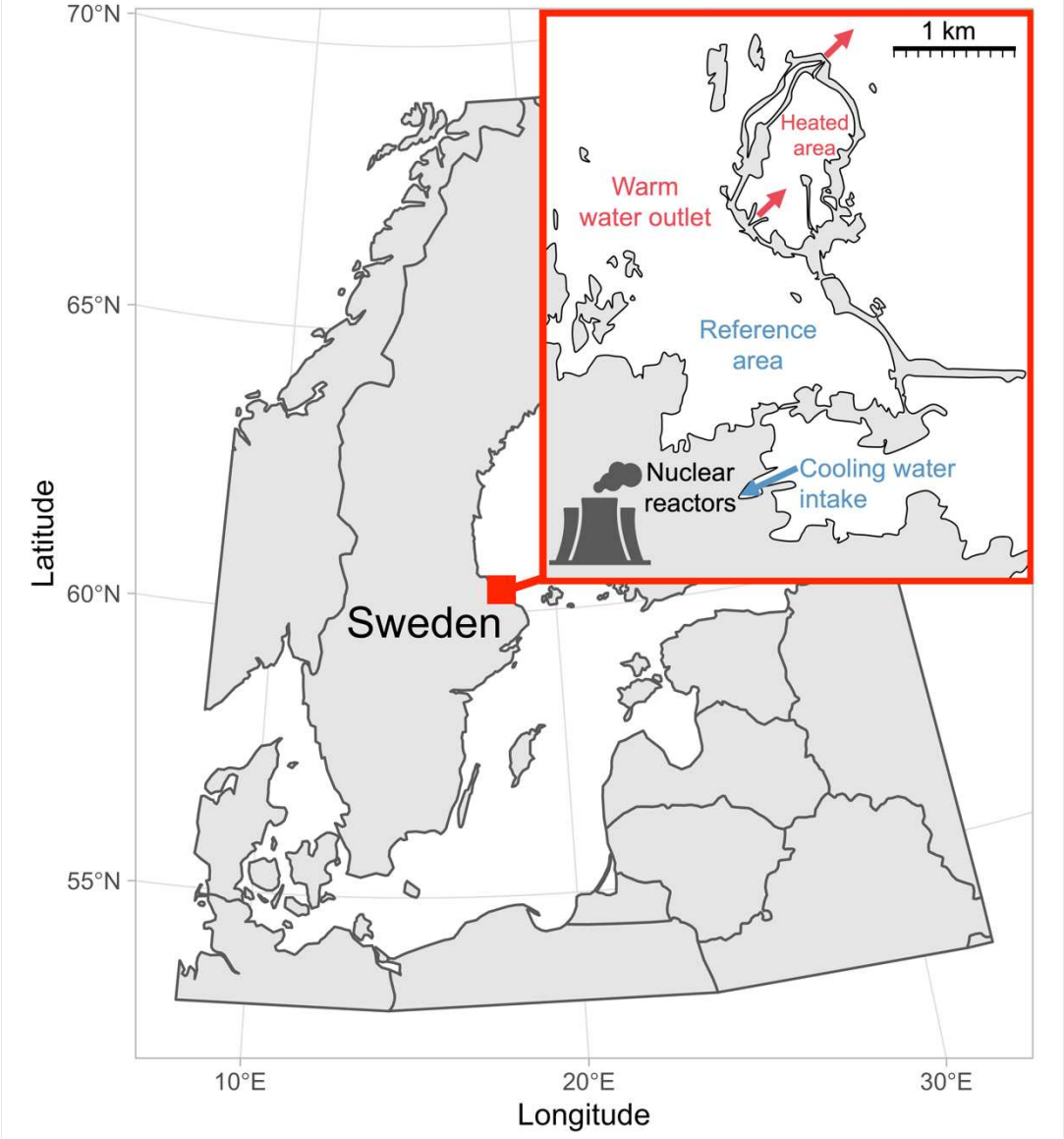

556

557 **Fig. 1.** Map of the area with the unique whole-ecosystem warming experiment from which
558 perch in this study was sampled. Inset shows the 1 km^2 enclosed coastal bay that has been
559 artificially heated for 23 years, the adjacent reference area with natural temperatures, and
560 locations of the cooling water intake and where the heated water outlet from nuclear power
561 plants enters the heated coastal basin.

562

563

564

565

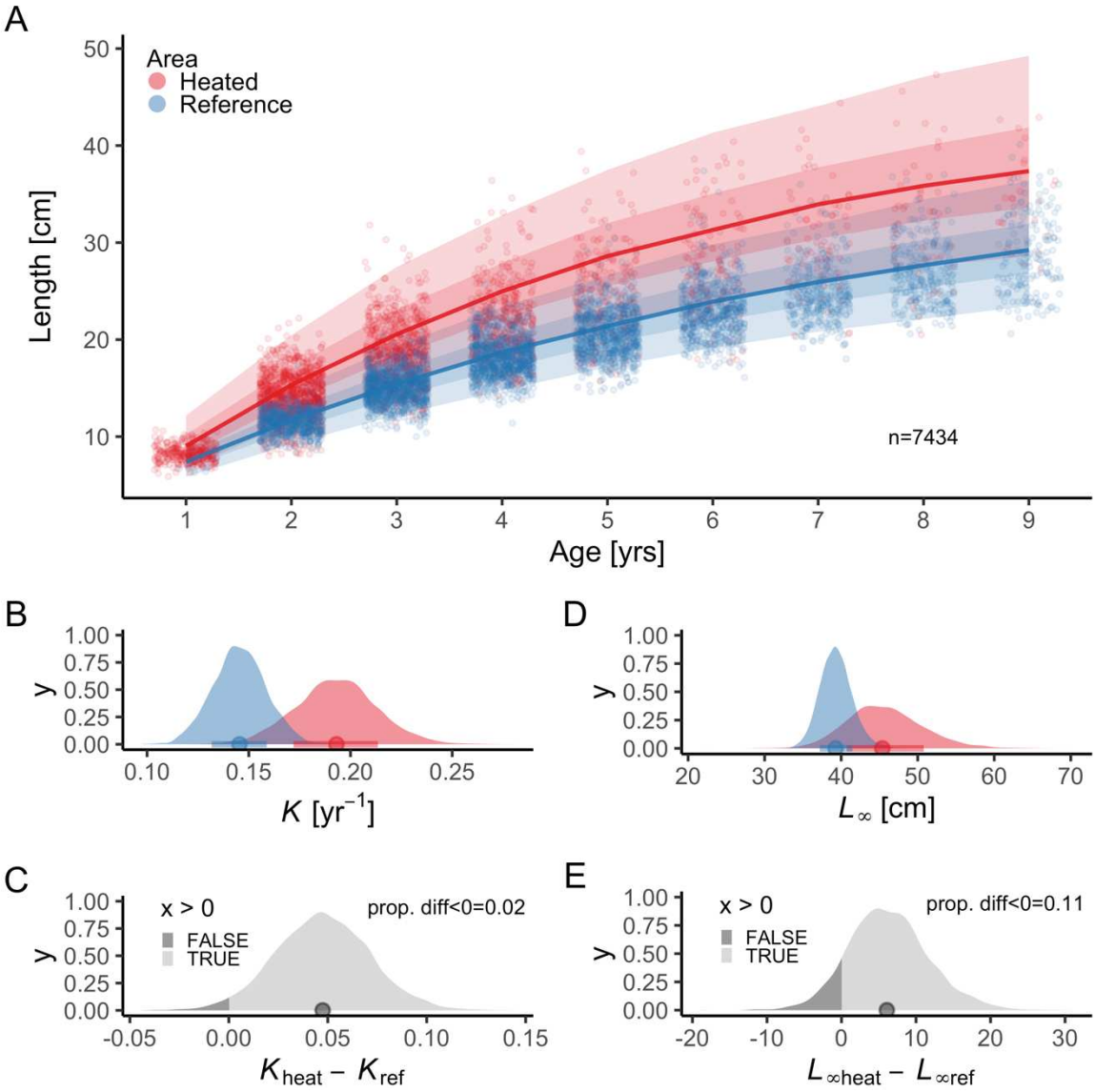

Fig. 2. Fish grow faster and reach larger sizes in the heated (red) enclosed bay compared to the reference (blue) area. Points in panel (A) depict individual-level length-at-age and lines show the global posterior prediction (both exponentiated) without group-level effects (i.e., cohort) from the von Bertalanffy growth model with area-specific coefficients. The shaded areas correspond to 50% and 90% credible intervals. Panel (B) shows the posterior distributions for growth coefficient (parameters K_{heat} (red) and K_{ref} (blue)) and (C) the distribution of their difference. Panel (D) shows the posterior distributions for asymptotic length (parameters $L_{\infty\mathrm{heat}}$ and $L_{\infty\mathrm{ref}}$), and (E) the distribution of their difference.

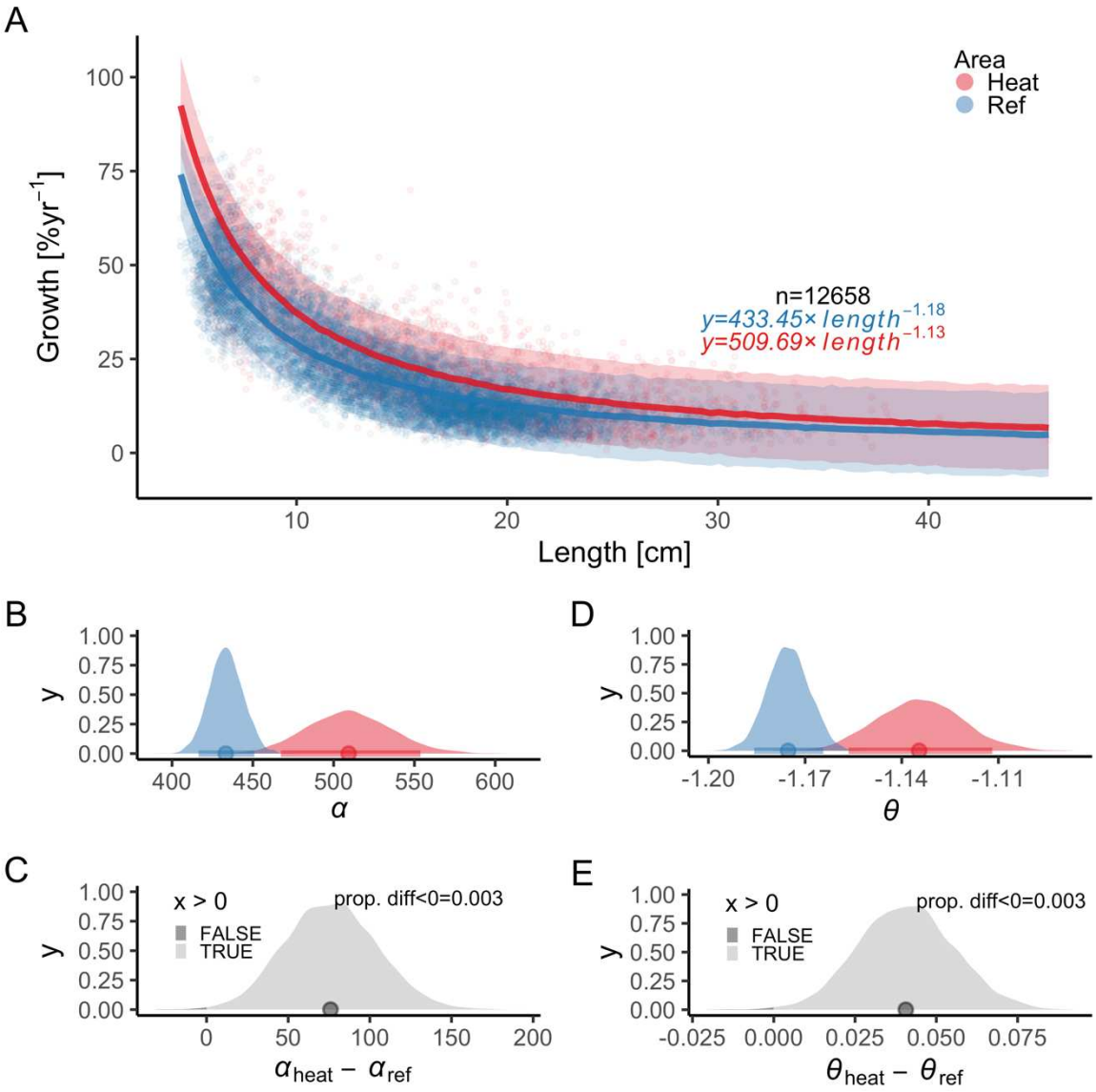

Fig. 3. The faster growth rates in the heated area (red) compared to the reference (blue) are maintained as fish grow. The points illustrate specific growth estimated from back-calculated length-at-age (within individuals) as a function of length (expressed as the geometric mean of the length at the start and end of the time interval). Lines show the global posterior prediction without group-level effects (i.e., individual within cohort) from the allometric growth model with area-specific coefficients. The shaded areas correspond to the 90% credible interval. The equation uses mean parameter estimates. Panel (B) shows the posterior distributions for initial growth (α_{heat} (red) and α_{ref} (blue)), and (C) the distribution of their difference. Panel (D) shows the posterior distributions for the allometric decline in growth with length (θ_{heat} and θ_{ref}), and (E) the distribution of their difference.

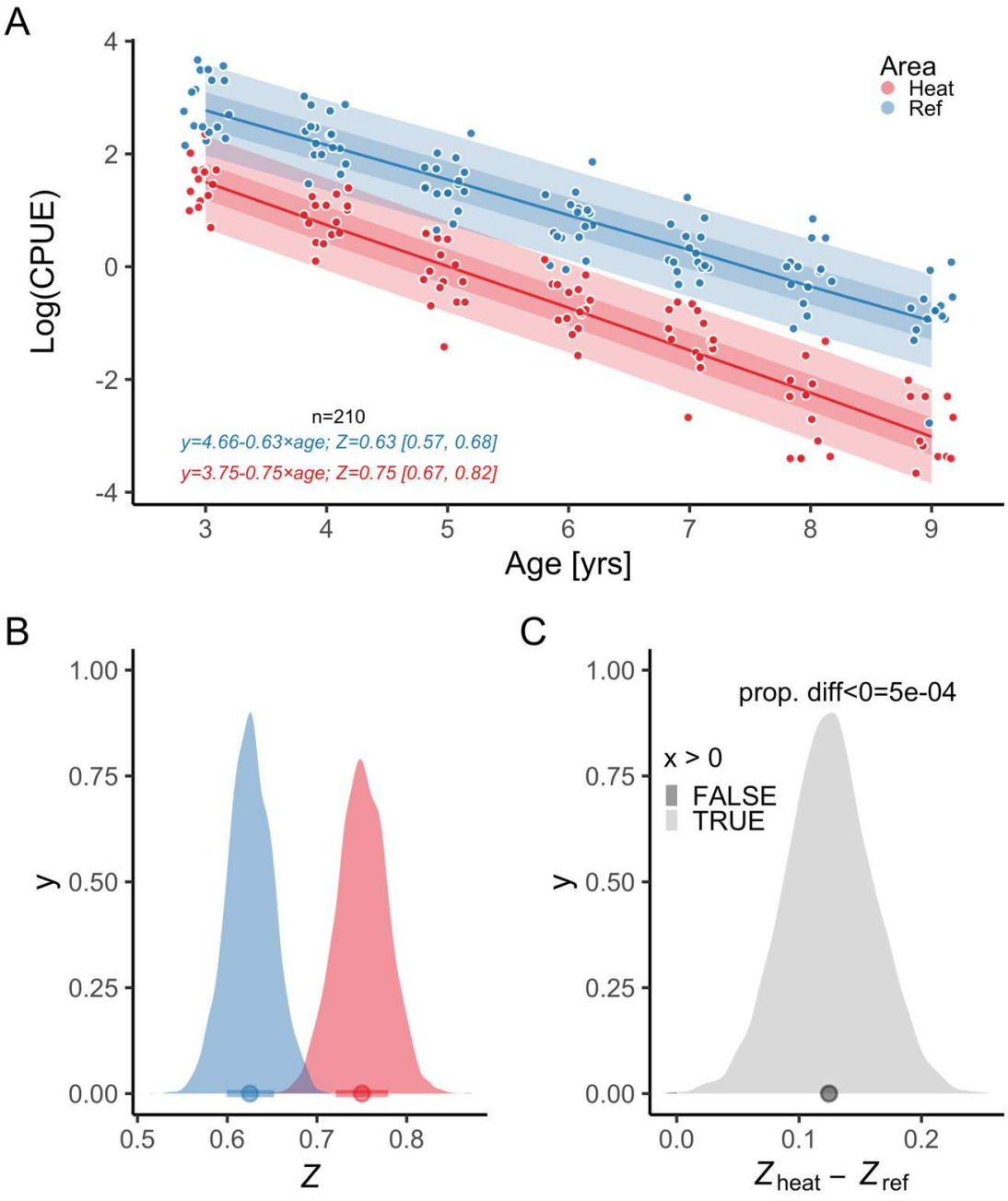

Fig. 4. The instantaneous mortality rate (Z) is higher in the heated area (red) than in the reference (blue). Panel (A) shows the $log\ (CPUE)$ as a function of age, where the slope corresponds to the global $-Z$. Lines show the posterior prediction without group-level effects (i.e., cohort) and the shaded areas correspond to the 50% and 90% credible intervals. The equation uses mean parameter estimates. Panel (B) shows the posterior distributions for mortality rate (Z_{heat} and Z_{ref}), and (C) the distribution of their difference.

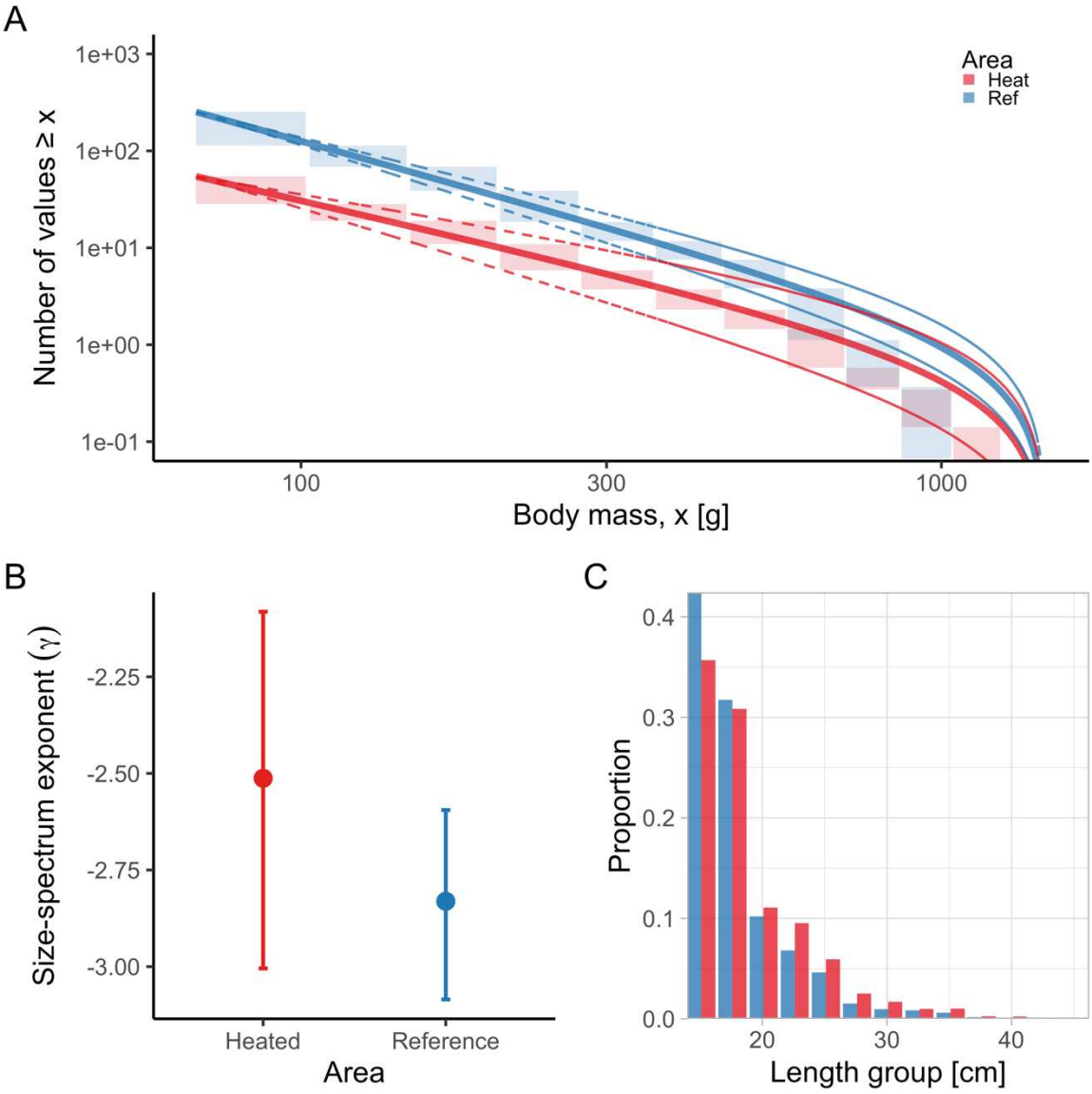

Fig. 5. The heated area (red) has a larger proportion of large fish than the reference area (blue), illustrated both in terms of the biomass size-spectrum (A), and histograms of proportions (C), but the difference in the slope of the size-spectra between the areas is not statistically clear (B). Panel (A) shows the size distribution and MLEbins fit (red and blue solid curve for the heated and reference area, respectively) with 95% confidence intervals indicated by dashed lines. The vertical span of rectangles illustrates the possible range of the number of individuals with body mass ≥ the body mass of individuals in that bin. Panel (B) shows the estimate of the size-spectrum exponent, γ, and vertical lines depict the 95% confidence interval. Panel (C) illustrates histograms of length groups in the heated and reference area as proportions (for all years pooled).